AGU PUBLICATIONS

Geophysical Research Letters

RESEARCH LETTER
10.1002/2014GL062474

Key Points:
- Tectonic stress modulates seepage along the Vestnesa Ridge in Fram Strait
- P-Cable 3-D seismic data reveal faults and fractures linked to seepage features
- Multiple seepage periods are recorded in gas chimneys for the last 2.7 Ma

Supporting Information:
- Figures S1 and S2

Correspondence to:
A. Plaza-Faverola,
andreia.a.faverola@uit.no

Citation:
Plaza-Faverola, A., S. Bünz, J. E. Johnson, S. Chand, J. Knies, J. Mienert, and P. Franek (2015), Role of tectonic stress in seepage evolution along the gas hydrate-charged Vestnesa Ridge, Fram Strait, *Geophys. Res. Lett.*, *42*, doi:10.1002/2014GL062474.

Received 8 NOV 2014
Accepted 8 JAN 2015
Accepted article online 13 JAN 2015

Role of tectonic stress in seepage evolution along the gas hydrate-charged Vestnesa Ridge, Fram Strait

A. Plaza-Faverola[1], S. Bünz[1], J. E. Johnson[1,2], S. Chand[1,3], J. Knies[1,3], J. Mienert[1], and P. Franek[1]

[1]Centre for Arctic Gas Hydrate, Environment and Climate, UiT The Arctic University of Norway, Tromsø, Norway, [2]Department of Earth Sciences, University of New Hampshire, Durham, New Hampshire, USA, [3]Geological Survey of Norway, Trondheim, Norway

Abstract Methane expulsion from the world ocean floor is a broadly observed phenomenon known to be episodic. Yet the processes that modulate seepage remain elusive. In the Arctic offshore west Svalbard, for instance, seepage at 200–400 m water depth may be explained by ocean temperature-controlled gas hydrate instabilities at the shelf break, but additional processes are required to explain seepage in permanently cold waters at depths >1000 m. We discuss the influence of tectonic stress on seepage evolution along the ~100 km long hydrate-bearing Vestnesa Ridge in Fram Strait. High-resolution P-Cable 3-D seismic data revealed fine-scale (>10 m width) near-vertical faults and fractures controlling seepage distribution. Gas chimneys record multiple seepage events coinciding with glacial intensification and active faulting. The faults document the influence of nearby tectonic stress fields in seepage evolution along this deepwater gas hydrate system for at least the last ~2.7 Ma.

1. Introduction

Methane emissions from ocean floors are a global phenomenon often recognized by the presence of seafloor morphologies (e.g., pockmarks and mounds) and acoustic flares, which indicate rising gas bubbles in the water column [e.g., *King and Maclean*, 1970]. Pockmark fields are frequently documented in gas hydrate provinces [e.g., *Vogt et al*., 1994; *Riedel et al*., 2002; *Hovland et al*., 2005; *Gay et al*., 2006; *Skarke et al*., 2014] as well as from shallow seafloors (<200 m) outside the gas hydrate stability zone (GHSZ) [e.g., *Hasiotis et al*., 1996; *Judd et al*., 2002; *García-García et al*., 2006; *Canet et al*., 2010; *Riboulot et al*., 2014]. The geological settings in which seepage has been identified vary from passive margins [e.g., *Berndt et al*., 2005], active pull-apart basins [e.g., *Canet et al*., 2010], subduction margins [e.g., *Barnes et al*., 2010], epicontinental seas [e.g., *Chand et al*., 2012], and mixed compressional and shear deformation regimes [e.g., *Plaza-Faverola et al*., 2014]. Seepage activity is episodic, and the duration of the episodes varies from short term (e.g., seasonal or tide related) to longer term (thousands of years) [e.g., *Hovland and Sommerville*, 1985; *Baraza and Ercilla*, 1996; *Hasiotis et al*., 1996; *Roberts and Carney*, 1997; *Çifçi et al*., 2003; *Moss et al*., 2012; *Plaza-Faverola et al*., 2012; *Crutchley et al*., 2013; *Pape et al*., 2014; *Riboulot et al*., 2014].

Identifying the processes controlling seepage distribution, periodicity, and duration is necessary to further understand the potential role of geological gas emissions on global climate. Episodic seepage at the updip termination of the GHSZ near the shelf break has been attributed to seasonal gas hydrate dissociation controlled by temperature variations [e.g., *Berndt et al*., 2014; *Phrampus and Hornbach*, 2012; *Skarke et al*., 2014; *Westbrook et al*., 2009]. Longer-term seepage periodicity (>10,000 years) has been attributed to pressure changes governed by processes associated with glacial-interglacial cycles like sea level fluctuations, changes in sedimentation rates, and ice loading/unloading [e.g., *Chand et al*., 2012; *Davy et al*., 2010; *Plaza-Faverola et al*., 2011; *Riboulot et al*., 2014] as well as fault reactivation mechanisms [e.g., *Plaza-Faverola et al*., 2014; *Roberts and Carney*, 1997; *Zühlsdorff and Spiess*, 2004]. Recent studies demonstrate the influence of inherited structural deformation, tectonic stresses, and fluid dynamics on modern margin evolution [*Autin et al*., 2013; *Zoback et al*., 1989; *Armitage et al*., 2010; *Terakawa et al*., 2013]. Tectonic stresses include the forces that drive or resist plate motion, forces that result from flexural deformation due to sediment loading, and inhomogeneous density distribution, as well as temperature-related forces from the cooling of oceanic lithosphere [*Zoback et al*., 1989].

Here our aim is to identify the processes controlling seepage evolution along Vestnesa Ridge, a contourite drift on the west Svalbard passive margin located in close proximity to the ultraslow-spreading ridges of the

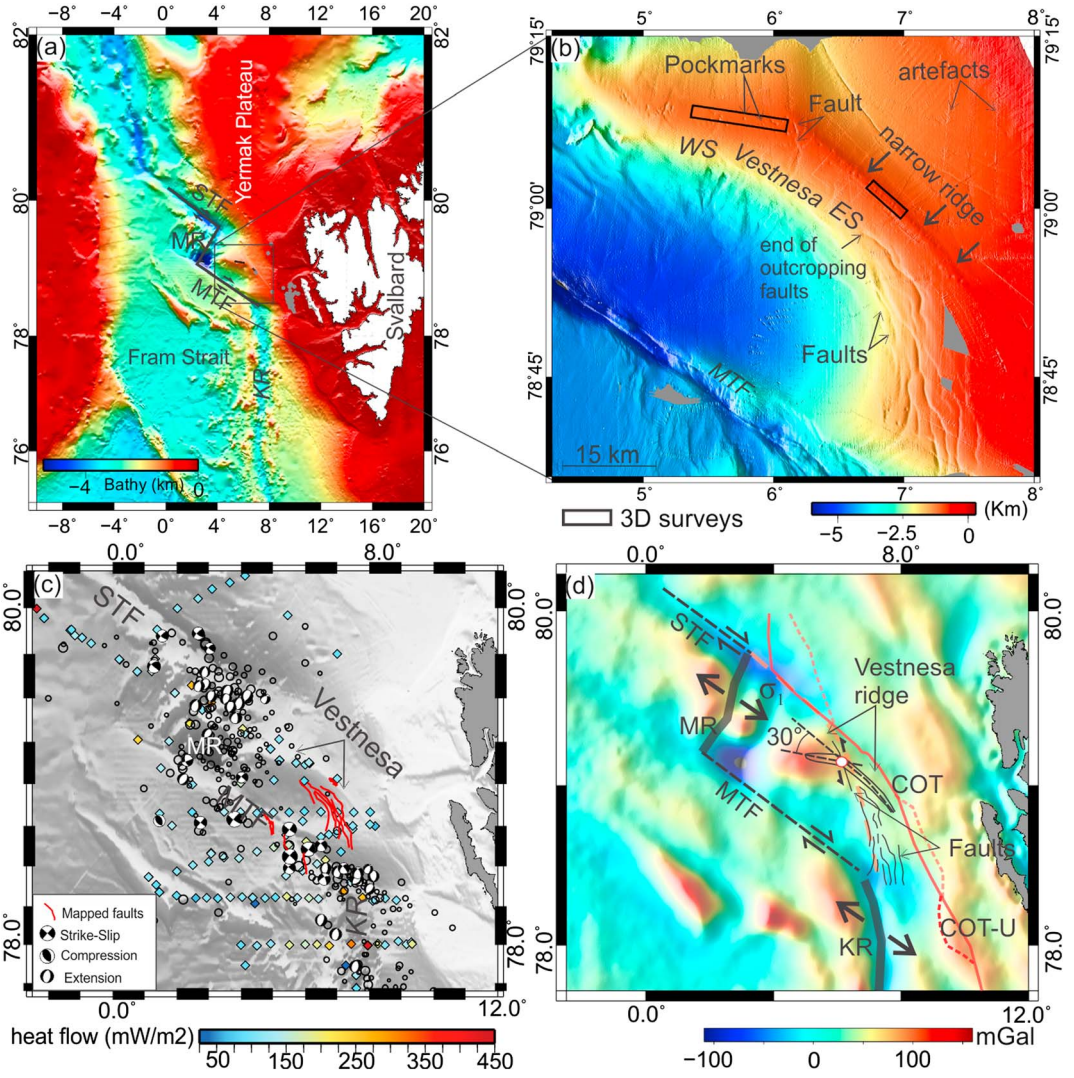

Figure 1. (a and b) Bathymetry maps showing location of Vestnesa Ridge and 3-D seismic surveys used in our study. MTF = Molloy Transform Fault, STF = Spitsbergen Transform Fault, MR = Molloy Ridge, and KR = Knipovich Ridge. The grey dots in Figure 1a are the mapped seep sites [*Sahling et al.*, 2014] at the west Svalbard margin. (c) Earthquake distribution (open circles) from 1964 to 2011, focal mechanisms (ISC, Reference Event Bulletin, hppt://www.isc.ac.uk), and heat flow data [*Crane et al.*, 1991; *Geissler et al.*, 2014] projected on the bathymetry. (d) Sketch of stress vectors influencing deformation on the Vestnesa Ridge, drawn over recently updated satellite gravity data (Scripps Institute of Oceanography (http://topex.ucsd.edu). Projected features are compiled from *Crane et al.* [2001], *Engen et al.* [2008], and *Hustoft et al.* [2009]. COT = continent-ocean transition and U = uncertain. The dashed orange line represents the weakness planes at the intersection between the STF and the northward extent of KR.

northern North Atlantic (Figure 1). Seepage along the west Svalbard margin occurs both inside and outside the extent of the hydrate stability zone. Seasonal hydrate dissociation is suggested to govern short-term seepage periodicity at the updip termination of the GHSZ in water depths <400 m [*Berndt et al.*, 2014; *Westbrook et al.*, 2009]. In deep waters (>1000 m), a gas hydrate province with associated seepage sites exists along the ~100 km long Vestnesa Ridge [*Bünz et al.*, 2012; *Hustoft et al.*, 2009; *Petersen et al.*, 2010; *Smith et al.*, 2014; *Vogt et al.*, 1994]. What controls the spatial distribution, duration, and periodicity of these deepwater seeps, however, remains elusive. We hypothesize that stresses associated with extension at the Molloy and Knipovich spreading ridges play a major role in seepage evolution along this hydrate system. We use high-resolution P-Cable 3-D seismic data to document stratigraphic and structural differences in the expression of fluid expulsion features along Vestnesa Ridge and subsequently propose a model for seepage evolution during the last 2.7 Ma.

2. Previous Research

The Vestnesa Ridge is a >2 km thick sediment drift developed off the west Svalbard margin, at water depths of 1000–2000 m, under the effect of contour currents [*Eiken and Hinz*, 1993; *Howe et al*., 2008; *Hustoft et al*., 2009; *Sarkar et al*., 2011]. It consists of two segments differing in strikes by ~30° [*Vogt et al*., 1994] (Figure 1). Although Vestnesa Ridge is part of the west Svalbard passive margin, it exists in a region with highly complex and currently active tectonics: the ridge is located between the dextral-slip Spitsbergen Transform Fault (STF) [*Ritzmann et al*., 2004] and the subparallel Molloy Transform Fault (MTF) [*Engen et al*., 2008] (Figure 1); the northward propagating Knipovich Ridge (KR) reaches the eastern Vestnesa segment from its south facing flank [*Crane et al*., 2001; *Vanneste et al*., 2005](Figure 1d). Based on Bouger gravity anomalies, the continent-ocean transition (COT) lies <20 km from Vestnesa's north facing flank [*Engen et al*., 2008]. Earthquake focal mechanisms show dextral strike-slip deformation to the north and the south and extension to the west and the southeast (Figure 1c). In addition, Vestnesa Ridge is located within the paleo-Spitsbergen shear zone, suggested to control orientation and distribution of extensional faults associated with rifting along the northern Knipovich Ridge [*Crane et al*., 1991, 2001]. The geological history of the region includes Paleocene strike slip within this ancient shear zone previous to the final breakup between Svalbard and Greenland [e.g., *Eldholm et al*., 1987]. Opening of Fram Strait dates from ~10 to 20 Ma [*Engen et al*., 2008; *Jakobsson et al*., 2007]. Heat flow measurements and regional seismic data [*Crane et al*., 1991; *Geissler et al*., 2014] (Figure 1c) revealed asymmetric opening of Fram Strait, suggested by *Crane et al*. [1991] to result from a combination of asymmetric pure shear, lithospheric simple shear, and rifting.

The Vestnesa Ridge is divided into three main stratigraphic sequences: YP1 (as for Yermak Plateau) is the oldest sequence (Miocene) and consists of synrift deposits over a <20 Ma old oceanic crust [*Eiken and Hinz*, 1993; *Hustoft et al*., 2009; *Ritzmann et al*., 2004], YP2 is the result of migrating contour currents with a main sedimentary depocenter striking parallel to the west Svalbard margin [*Eiken and Hinz*, 1993], and YP3, also dominated by margin-parallel contour currents, has two main depocenters separated by a thin sedimentary sequence [*Eiken and Hinz*, 1993]. The YP2/YP3 boundary is dated to ~2.7 Ma based on correlations with Ocean Drilling Program (ODP) Leg 151 sites [*Knies et al*., 2009, 2014; *Mattingsdal et al*., 2014].

3. Data and Methods

We used two high-resolution 3-D seismic data sets acquired with the P-Cable system [*Planke et al*., 2009] on board R/V *Helmer Hanssen* (i.e., $1.8 \times 15\ km^2$ and $2 \times 7\ km^2$) (Figure 1b). Acquisition and processing details for data on the western segment can be found in *Petersen et al*. [2010]. Data from the eastern segment were acquired during the summer in 2013 using 14 25 m long streamers with eight channels per streamer. The source consisted of a mini-GI gun ($246/246\ cm^3$) firing every 6 s with a peak frequency of 135 Hz. Data processing included band-pass filtering (30-50-300-350 Hz), amplitude correction, and common depth point reflection binning at $6.25 \times 6.25\ m^2$. Normal moveout correction, stacking, and 3-D Stolt migration were done using 1500 m/s. The migrated stack has a lateral resolution of 6.25 m and a vertical resolution of ~5 m (i.e., taken as $\lambda/2$).

Variance maps—a measurement of dip and azimuth variability of adjacent seismic traces— were extracted along major reflections for structural analysis. Faults were automatically extracted for dip and azimuth quantifications using commercially available seismic interpretation software. Seismic results were analyzed in conjunction with high-resolution bathymetry data (50×50 m) [*Hustoft et al*., 2009; *Vanneste et al*., 2005], seismological data (International Seismological Centre (ISC) database http://www.isc.ac.uk), and updated gravimetric maps (Scripps Institute of Oceanography http://topex.ucsd.edu).

4. Observations and Discussion

The following sections describe and discuss the structural and stratigraphic observations that allow us to reconstruct the seepage evolution along Vestnesa Ridge and enable us to identify major processes modulating gas expulsion along this deepwater gas hydrate system.

4.1. Faulting and Fracturing of Vestnesa Ridge

The area connecting the southern rim of Vestnesa Ridge with Knipovich Ridge (KR) hosts a system of westward dipping extensional faults visible on multibeam bathymetry and seismic data [*Crane et al*., 2001; *Hustoft et al*., 2009; *Vanneste et al*., 2005]. The faults strike NNW-SSE toward the KR spreading center but change to a NW-SE

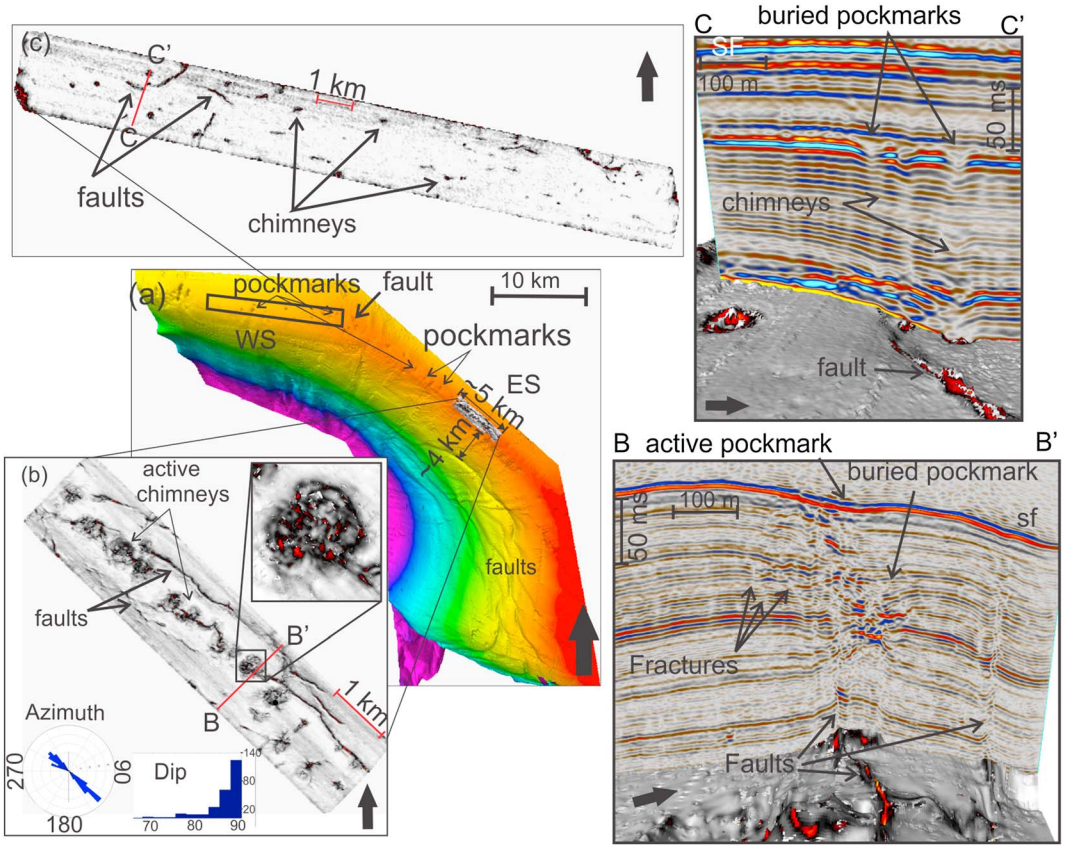

Figure 2. Bathymetry map along (a) Vestnesa Ridge showing orientation of outcropping regional faults with respect to the mapped (b and c) subseabed faults in 3-D seismic data. Structural maps (Figures 2b and 2c) were extracted along seismic horizon H80 (~1.5 Ma [*Mattingsdal et al.*, 2014]) at both eastern and western segments of Vestnesa Ridge. B-B′ and C-C′ show the seismic character of chimneys at each segment. The inset in Figure 2b is a detailed view of the internal structure of a chimney (fine-scale polygonal fracturing). For geographical location of the seismic volumes, please refer to Figure 1.

strike at the rim of the eastern Vestnesa segment, where they no longer have a bathymetric expression (Figures 1b and 3a). Although the NW-SE trending faults are not visible on multibeam bathymetry at the crest of the ridge, 3-D seismic data reveal fine-scale (~10 m width), NW-SE oriented ($300 < \text{azimuth} < 330$; Figure 3b) curvilinear faults (i.e., with gentle normal throws, ~5–10 m) and fractures (i.e., near-vertical features with no evident vertical displacement) (Figures 2b and 4). Only some of these faults have a subtle manifestation at the seafloor, indicating recent activity (Figures 3 and 4). Their orientation and curvilinear character, mainly at the eastern Vestnesa segment, make them comparable to the seafloor emergent fault system south of Vestnesa (Figures 2a and 2b), interpreted as evidence of ongoing northward propagation of KR [*Crane et al.*, 2001; *Vanneste et al.*, 2005]. However, these features at the eastern Vestnesa segment are near vertical and dipping NE at $>60°$ (Figure 2b), opposite dip to the emergent extensional faults north of KR [*Hustoft et al.*, 2009].We suggest that these features are thus associated with shear deformation [e.g., *Sylvester*, 1988]. Similar scale faults have been recently documented in P-Cable seismic data from the Hikurangi Margin, where seepage systems were suggested to be associated with Riedel shears [*Plaza-Faverola et al.*, 2014]. An interpretation of NW-SE oriented shear-related faults dissecting the Vestnesa Ridge with an extensional component supports the mixed simple and pure shear model proposed by *Crane et al.* [2001] for the opening of Fram Strait.

The faulting pattern at the eastern Vestnesa segment is distinctive. The 3-D seismic data from the western Vestnesa segment show discontinuous fault segments, which appear less defined in the seismic data (Figure 2c). NS to NW-SE oriented faults cut Vestnesa Ridge between the two segments (Figures 1b and 2b). This fault area is aligned with the northwest termination of extensional faults propagating from KR [*Crane et al.*, 2001] and connects to the north with the projected continent-ocean transition (COT) [*Ritzmann et al.*, 2004; *Engen et al.*, 2008] (Figure 1d). Based on this observation, we infer the presence of a shear weakness

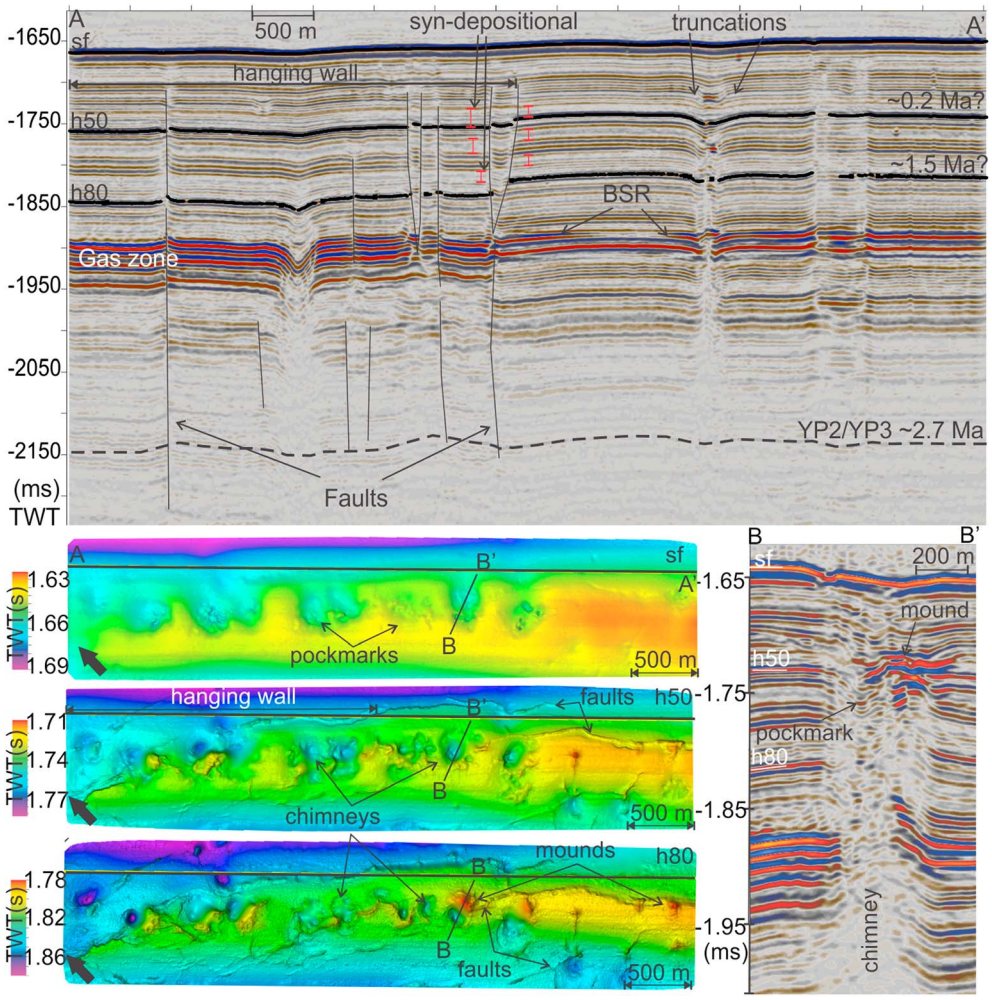

Figure 3. Seismic profile in two-way time showing syndepositional faulting and fracturing imaged at the eastern Vestnesa segment. Three time maps (sf–seafloor, H50 and H80) are presented to show variations in the morphology of gas chimneys through time and their spatial relation to faults. The inset shows an example of a mound adjacent to a buried pockmark along a fault.

plane between the two Vestnesa Ridge segments (Figure 1d) coinciding with a zone where the southward extent of the Spitsbergen Transform Fault (STF) (i.e., following the flow line of Greenland relative to Eurasia [*Engen et al*., 2008]) and the northward propagating KR [*Crane et al*., 2001] encounters each other (Figure 1d). This hypothesis is further supported by gravimetric maps (Scripps Institute of Oceanography http://topex.ucsd.edu) in which a remarkably high gravity anomaly marks a distinction between the western and eastern Vestnesa segments (Figure 1d). We speculate that a component of the Molloy Ridge southeast trending stress vector is accommodated along the N-S oriented weakness plane between ridge segments, resulting in strike-slip movement along the weakness plane, translating the western Vestnesa Ridge segment southward (Figure 1d). With a Molloy Ridge (MR) stress vector approximately parallel to the eastern Vestnesa segment, at an incidence angle of ~30° with respect to the western segment (Figure 1d) and a half-spread rate of 6.5 mm/yr [*Ehlers and Jokat*, 2009], the tectonic stress from MR can be partitioned to yield a rate of southward slip of the western Vestnesa segment of ~3.7 mm/yr.

These structural differences along Vestnesa Ridge (Figure 1d) may be reflecting lateral variations in the strength and elastic properties of the strata [e.g., *Zoback et al*., 1989] or may result from heterogeneities in the stress field [*Hardebeck and Hauksson*, 2001; *Luther and Axen*, 2013]. Temporal and spatial variations of stress fields are expected in seismically active regions [*Hardebeck and Hauksson*, 2001; *Luther and Axen*, 2013, and references therein]. We argue that although the entire ridge is under the influence of insipient shear,

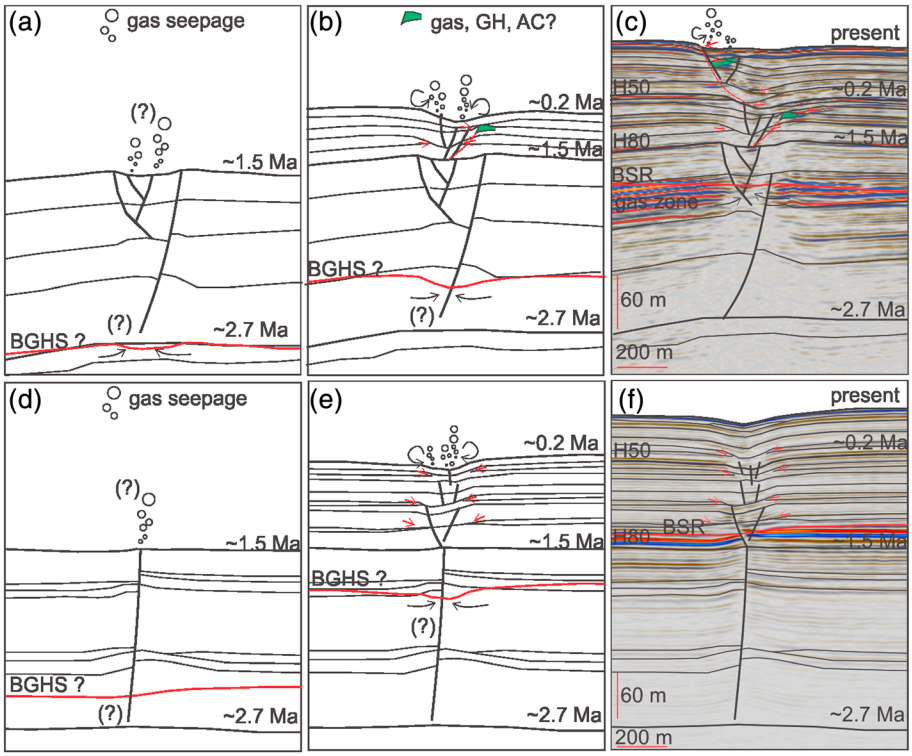

Figure 4. Comparison between the seepage evolution at (a–c) the eastern and (d–f) western Vestnesa segments. BGHS = base of the gas hydrate stability zone and BSR = bottom simulating reflector.

i.e., from the STF [e.g., *Crane et al.*, 2001], each Vestnesa Ridge segment reflects the influence of different stress fields. The western Vestnesa segment is dominantly affected by southward slip motion at present. The orientation of the MR spreading vector with respect to the eastern Vestnesa segment (i.e., acting as σ_1) may be favoring strike-slip faulting and explains the presence of recently active faults and fractures at the eastern segment (Figure 2b). These faults could have enhanced permeability [e.g., *Roberts et al.*, 1996] and explain the seafloor seepage exclusively observed in this part of Vestnesa Ridge at present.

4.2. Chimney Morphology and Distribution Along Vestnesa Ridge

Gas chimneys underlying seafloor pockmarks are documented from both the western [*Petersen et al.*, 2010] and eastern Vestnesa segments (Figure 2). The 3-D seismic data reveal noteworthy differences in the spatial distribution, morphology, and geometry of chimneys along the ridge [*Bünz et al.*, 2012]. While the eastern segment crest is narrow (<2 km wide), rectilinear, and has active seepage, the western segment has a broad (~4 km wide) crest where acoustic flares have not been documented [*Bünz et al.*, 2012; *Smith et al.*, 2014].

Importantly, gas chimneys, regardless of their position along the ridge, show evidence of buried pockmarks or mounds (i.e., indicators of paleoseepage) [*Plaza-Faverola et al.*, 2011; *Riboulot et al.*, 2014] identified by truncation of reflections through chimney conduits at specific stratigraphic intervals (Figures 3 and 4). Nonetheless, the internal geometry of chimneys at each Vestnesa segment suggests dissimilar seepage evolution (Figures 3 and 4). At the western segment, gas chimneys consist of concentric stacks of pockmarks with symmetric truncations with respect to chimney centers (Figures 4d–4f). These chimneys are similar to those documented at other inactive pockmark fields, e.g., at the mid-Norwegian margin [*Plaza-Faverola et al.*, 2011]. At the eastern Vestnesa segment, pockmark stacks are nonconcentric, chimneys have a crooked geometry, they record syndepositional deformation, and their latest stage of deformation occurred such that truncation of reflections prograded along an oblique plane (Figures 4a–4c). Buried mounds, suggested for other margins to indicate authigenic carbonate precipitation during past seepage events [e.g., *Plaza-Faverola et al.*, 2011], are also a dominant characteristic of these chimneys (Figure 3).

In terms of their distribution, gas chimneys are directly linked to fault planes (Figures 2b, 2c, and 4). Gas accumulation at the crest of Vestnesa Ridge is morphologically controlled [*Bünz et al*., 2012]. This factor together with the presence of faults and fractures as pathways for fluid migration determines the gas chimney distribution (Figures 2b and 4). The relationship between chimney evolution and faulting is clearer at the eastern Vestnesa segment, where currently active seepage [*Bünz et al*., 2012; *Smith et al*., 2014] is occurring along interpreted shear-related faults (as described in section 4.1). This assumption is further based on the observation of short (<10 m) syndepositional fault offsets indicating fault reactivation (Figure 3), as well as the presence of high seismic amplitude anomalies, highly disrupted strata, and buried mounds (Figure 3), indicating active fluid accumulation and migration exclusively at the eastern Vestnesa segment. The westward decrease in fault continuity along the ridge (Figure 3) coincides with a decrease in seepage activity and is consistent with our interpretation of faults with higher permeability (i.e., presently more active) in the eastern, compared to the western, Vestnesa segment.

4.3. Chronostratigraphic Constraints for the Last 2.7 Ma of Seepage

Correlation of our seismic data with seismic stratigraphy from the Yermak Plateau [*Mattingsdal et al*., 2014] places the YP3/YP2 interface (~2.7 Ma) >250 m below the bottom simulating reflector (BSR) in the region and shows that a reflection dated to ~1.5 Ma [*Mattingsdal et al*., 2014] corresponds to a major reflection in our data, identified as H80 (Figures 3 and 4). The 2.7 Ma interface marks the intensification of Northern Hemisphere Plio-Pleistocene glaciations, while the 1.5 Ma interface marks a regional glacial intensification at the west Svalbard margin [*Knies et al*., 2009; *Mattingsdal et al*., 2014; *Vorren and Laberg*, 1997]. An additional major seismic reflection (H50; Figures 3 and 5) is estimated to be ~0.2–0.3 Ma based on average sedimentation rates extrapolated from ODP (Ocean Drilling Program) sites in the Yermak Plateau [*Mattingsdal et al*., 2014] and a gravity core at the western Vestnesa segment [*Consolaro et al*., 2014]. Gas chimneys record morphological changes through these three major stratigraphic periods (Figure 4):

1. *2.7–1.5 Ma*: Active faulting preceded the formation of gas chimneys with possible seafloor seepage associated (Figures 4a and 4d).
2. *1.5–~0.2 Ma*: A stack of concentric pockmarks intercalated with periods of inactivity marks the onset of regular seepage cycles (Figures 4b and 4e). Observation of stacked pockmarks only posterior to 1.5 Ma coincides with a period of glacial intensification and repeated ice sheet advances beyond the shelf edge [*Knies et al*., 2009]. Fault reactivation and syndepositional deformation including buried mounds (Figure 2, B-B′) toward the eastern segment dominate this period.
3. *~0.2 Ma to present*: This is the second and youngest major stack of pockmarks and mounds. Toward the western segment, short-lived (<1000 years) periodic seepage events [*Consolaro et al*., 2014] are manifested as concentrically stacked pockmarks, largely inactive at present (Figure 4f). Toward the eastern segment, this period is characterized by an oblique progradation of buried pockmark (Figures 4c and 4f) that record syndepositional faulting events and active seepage [*Smith et al*., 2014].

4.4. Seepage Modulation

Based on the presented structural and stratigraphic observations, we argue that gas chimneys along both Vestnesa segments record periodic seepage cycles overlapped by less predictable seepage events recorded primarily within the active fault-related chimneys in the eastern Vestnesa segment (Figure 4c). In our model of seepage evolution, gas expulsion events are dominated by pressure changes (i.e., that have a direct effect on the dynamics of the free gas zone underneath the hydrate zone [*Bünz et al*., 2012; *Petersen et al*., 2010; *Hustoft et al*., 2009]) and/or fault movements.

Several processes could explain fault reactivation-driven seepage events along Vestnesa Ridge: (1) increases in sediment input (e.g., reflecting sedimentation rate changes during buildup of the contourite drift [*Eiken and Hinz*, 1993]); (2) sea level fluctuations between glaciations, as observed in the Gulf of Mexico [*Roberts and Carney*, 1997]; and (3) seismicity as a cause and/or effect of changes in the stress field [e.g., *Luther and Axen*, 2013] involving active rifting and shear motion surrounding Vestnesa (Figure 1c). Tectonic stress induces rapid buildup of excess pore fluid pressure and the subsequent flow of fluids through faults, triggering fault movement, fracturing, and seismicity [*Sibson*, 1990; *Terakawa et al*., 2013]. Polygonal-like fractures successfully imaged within some of the chimneys linked to active faults (Figure 2b, inset) might provide

evidence of excess pore fluid pressure cycles associated with faulting [e.g., *Gay et al*., 2012; *Osborne and Swarbrick*, 1997; *Sibson*, 2000; *Roberts et al*., 1996].

For resolving the causes of more regular seepage, improved chronostratigraphic constraints for the Pleistocene glacial-interglacial periods are needed locally at Vestnesa Ridge. Nevertheless, its manifestation as stacked pockmarks intercalated with the periods of inactivity (Figure 4) makes these fluid escape features comparable to those from the mid-Norwegian margin, the Hikurangi Margin, Congo Basin, and the Gulf of Lions, where a link between periodicity and glacial-interglacial cycles has been documented [e.g., *Andresen and Huuse*, 2011; *Davy et al*., 2010; *Riboulot et al*., 2014; *Plaza-Faverola et al*., 2011].

Finally, the Vestnesa Ridge gas hydrate system, similar to other gas-charged contourite drifts such as Blake Ridge offshore the U.S. coast, evolved under cold deepwater conditions (>1000 m). This characteristic implies (1) that the extent of the GHSZ is less vulnerable to temperature changes and is more pressure dominated; (2) that gas recycling from hydrate dissociation at the base of the GHSZ—and not at the seafloor—is an important process caused by the small-scale fluctuation of the GHSZ extent, sustaining periodic seepage through faults and fractures; and (3) that at every fault movement, free gas trapped at the base of the GHSZ, is available to be released in response to tectonic stresses.

5. Conclusions

High-resolution P-Cable 3-D seismic data from the ~100 km long hydrate-charged Vestnesa Ridge in Fram Strait revealed faults and fractures that reflect the influence of nearby tectonic stress fields (i.e., rifting at the Molloy and Knipovich Ridges, as well as shear motion along the Spitsbergen Transform Fault) on seepage evolution. Gas chimney distribution and seepage periodicity appear closely linked to these faults and fractures. Multiple seepage periods during the last 2.7 Ma have been identified. Periodic seepage on the order of a few hundred thousand years is suggested by regular intervals of buried pockmarks coinciding with glacial intensification at the west Svalbard margin. Additional irregular gas expulsion events, likely associated with fault reactivation and fracturing, are identified from syndepositional fault deformation within gas chimneys. Vestnesa Ridge hosts a deepwater gas hydrate system with significant amounts of gas trapped underneath that has been susceptible to gas expulsion in response to mechanical failure induced by tectonic stress.

Acknowledgments
The research is funded by the Norwegian Research Council through CAGE-Center for Arctic Gas Hydrate, Environment and Climate (grant 223259). We thank the crew of R/V *Helmer Hanssen* and those who contributed to P-Cable data acquisition. We acknowledge the use of GEBCO and IBCAO bathymetry grids, seismological data from ISC, gravity data from SIO, as well as Schlumberger interpretation software. We are thankful to Kathleen Crane for her feedback and suggestions.

The Editor thanks David Mosher and an anonymous reviewer for their assistance in evaluating this paper.

References

Andresen, K. J., and M. Huuse (2011), 'Bulls-eye'pockmarks and polygonal faulting in the Lower Congo Basin: Relative timing and implications for fluid expulsion during shallow burial, *Mar. Geol.*, *279*(1), 111–127.

Armitage, J. J., J. S. Collier, and T. A. Minshull (2010), The importance of rift history for volcanic margin formation, *Nature*, *465*(7300), 913–917.

Autin, J., N. Bellahsen, S. Leroy, L. Husson, M.-O. Beslier, and E. d'Acremont (2013), The role of structural inheritance in oblique rifting: Insights from analogue models and application to the Gulf of Aden, *Tectonophysics*, *607*, 51–64.

Baraza, J., and G. Ercilla (1996), Gas-charged sediments and large pockmark-like features on the Gulf of Cadiz slope (SW Spain), *Mar. Pet. Geol.*, *13*(2), 253–261.

Barnes, P., G. Lamarche, J. Bialas, S. Henrys, I. Pecher, G. L. Netzeband, J. Greinert, J. J. Mountjoy, K. Pedley, and G. Crutchley (2010), Tectonic and geological framework for gas hydrates and cold seeps on the Hikurangi subduction margin, New Zealand, *Mar. Geol.*, *272*(1), 26–48.

Berndt, C., J. Mienert, M. Vanneste, and S. Bunz (2005), Gas hydrate dissociation and sea-floor collapse in the wake of the Storegga Slide, Norway Onshore-Offshore Relationships on the North Atlantic Margin, *Norw. Petrol. Soc. Spec. Publ.*, *12*, 285–292.

Berndt, C., T. Feseker, T. Treude, S. Krastel, V. Liebetrau, H. Niemann, V. J. Bertics, I. Dumke, K. Dünnbier, and B. Ferré (2014), Temporal constraints on hydrate-controlled methane seepage off Svalbard, *Science*, *343*(6168), 284–287.

Bünz, S., S. Polyanov, S. Vadakkepuliyambatta, C. Consolaro, and J. Mienert (2012), Active gas venting through hydrate-bearing sediments on the Vestnesa Ridge, offshore W-Svalbard, *Mar. Geol.*, *332*, 189–197.

Canet, C., R. M. Prol-Ledesma, P. R. Dando, V. Vázquez-Figueroa, E. Shumilin, E. Birosta, A. Sánchez, C. J. Robinson, A. Camprubí, and E. Tauler (2010), Discovery of massive seafloor gas seepage along the Wagner Fault, northern Gulf of California, *Sediment. Geol.*, *228*(3), 292–303.

Chand, S., T. Thorsnes, L. Rise, H. Brunstad, D. Stoddart, R. Bøe, P. Lågstad, and T. Svolsbru (2012), Multiple episodes of fluid flow in the SW Barents Sea (Loppa High) evidenced by gas flares, pockmarks and gas hydrate accumulation, *Earth Planet. Sci. Lett.*, *331*, 305–314.

Çifçi, G., D. Dondurur, and M. Ergün (2003), Deep and shallow structures of large pockmarks in the Turkish shelf, Eastern Black Sea, *Geo Mar. Lett.*, *23*(3–4), 311–322.

Consolaro, C., T. Rasmussen, G. Panieri, J. Mienert, S. Bünz, and K. Sztybor (2014), Carbon isotope ($\delta^{13}C$) excursions suggest times of major methane release during the last 14 ka in Fram Strait, the deep-water gateway to the Arctic, *Clim. Past Discuss.*, *10*(5), 4191–4227.

Crane, K., E. Sundvor, R. Buck, and F. Martinez (1991), Rifting in the northern Norwegian-Greenland Sea: Thermal tests of asymmetric spreading, *J. Geophys. Res.*, *96*(B9), 14,529–14,550, doi:10.1029/91JB01231.

Crane, K., H. Doss, P. Vogt, E. Sundvor, G. Cherkashov, I. Poroshina, and D. Joseph (2001), The role of the Spitsbergen shear zone in determining morphology, segmentation and evolution of the Knipovich Ridge, *Mar. Geophys. Res.*, *22*(3), 153–205.

Crutchley, G. J., C. Berndt, S. Geiger, D. Klaeschen, C. Papenberg, I. Klaucke, M. J. Hornbach, N. L. Bangs, and C. Maier (2013), Drivers of focused fluid flow and methane seepage at south Hydrate Ridge, offshore Oregon, USA, *Geology*, *41*(5), 551–554.

Davy, B., I. Pecher, R. Wood, L. Carter, and K. Gohl (2010), Gas escape features off New Zealand: Evidence of massive release of methane from hydrates, *Geophys. Res. Lett.*, *37*, L21309, doi:10.1029/2010GL045184.
Ehlers, B.-M., and W. Jokat (2009), Subsidence and crustal roughness of ultra-slow spreading ridges in the northern North Atlantic and the Arctic Ocean, *Geophys. J. Int.*, *177*(2), 451–462.
Eiken, O., and K. Hinz (1993), Contourites in the Fram Strait, *Sediment. Geol.*, *82*(1), 15–32.
Eldholm, O., J. I. Faleide, and A. M. Myhre (1987), Continent-ocean transition at the western Barents Sea/Svalbard continental margin, *Geology*, *15*(12), 1118–1122.
Engen, Ø., J. I. Faleide, and T. K. Dyreng (2008), Opening of the Fram Strait gateway: A review of plate tectonic constraints, *Tectonophysics*, *450*(1), 51–69.
García-García, A., D. Orange, T. Lorenson, O. Radakovitch, T. Tesi, S. Miserocchi, S. Berne, P. Friend, C. Nittrouer, and A. Normand (2006), Shallow gas off the Rhône prodelta, Gulf of Lions, *Mar. Geol.*, *234*(1), 215–231.
Gay, A., M. Lopez, P. Cochonat, M. Seranne, D. Levache, and G. Sermondadaz (2006), Isolated seafloor pockmarks linked to BSRs, fluid chimneys, polygonal faults and stacked Oligocene-Miocene turbiditic palaeochannels in the Lower Congo Basin, *Mar. Geol.*, *226*(1–2), 25–40.
Gay, A., R. Mourgues, C. Berndt, D. Bureau, S. Planke, D. Laurent, S. Gautier, C. Lauer, and D. Loggia (2012), Anatomy of a fluid pipe in the Norway Basin: Initiation, propagation and 3D shape, *Mar. Geol.*, *332–334*(0), 75–88.
Geissler, W. H., P. V. Pulm, W. Jokat, and A. C. Gebhardt (2014), Indications for the occurrence of gas hydrates in the Fram Strait from heat flow and multichannel seismic reflection data, *J. Geol. Res. Solid Earth*, doi:10.1155/2014/582424.
Hardebeck, J. L., and E. Hauksson (2001), Crustal stress field in southern California and its implications for fault mechanics, *J. Geophys. Res.*, *106*(B10), 21,859–21,882, doi:10.1029/2001JB000292.
Hasiotis, T., G. Papatheodorou, N. Kastanos, and G. Ferentinos (1996), A pockmark field in the Patras Gulf (Greece) and its activation during the 14/7/93 seismic event, *Mar. Geol.*, *130*(3), 333–344.
Hovland, M., and J. H. Sommerville (1985), Characteristics of two natural gas seepages in the North Sea, *Mar. Pet. Geol.*, *2*(4), 319–326.
Hovland, M., H. Svensen, C. F. Forsberg, H. Johansen, C. Fichler, J. H. Fossa, R. Jonsson, and H. Rueslatten (2005), Complex pockmarks with carbonate-ridges off mid-Norway: Products of sediment degassing, *Mar. Geol.*, *218*(1–4), 191–206.
Howe, J. A., T. M. Shimmield, R. Harland, and N. Eyles (2008), Late Quaternary contourites and glaciomarine sedimentation in the Fram Strait, *Sedimentology*, *55*(1), 179–200.
Hustoft, S., S. Bunz, J. Mienert, and S. Chand (2009), Gas hydrate reservoir and active methane-venting province in sediments on $<$20 Ma young oceanic crust in the Fram Strait, offshore NW Svalbard, *Earth Planet. Sci. Lett.*, *284*(1–2), 12–24.
Jakobsson, M., J. Backman, B. Rudels, J. Nycander, M. Frank, L. Mayer, W. Jokat, F. Sangiorgi, M. O'Regan, and H. Brinkhuis (2007), The early Miocene onset of a ventilated circulation regime in the Arctic Ocean, *Nature*, *447*(7147), 986–990.
Judd, A. G., R. Sim, P. Kingston, and J. McNally (2002), Gas seepage on an intertidal site: Torry Bay, Firth of Forth, Scotland, *Cont. Shelf Res.*, *22*(16), 2317–2331.
King, L. H., and B. Maclean (1970), Pockmarks on Scotian Shelf, *Geol. Soc. Am. Bull.*, *81*(10), 3141–3148.
Knies, J., J. Matthiessen, C. Vogt, J. S. Laberg, B. O. Hjelstuen, M. Smelror, E. Larsen, K. Andreassen, T. Eidvin, and T. O. Vorren (2009), The Plio-Pleistocene glaciation of the Barents Sea–Svalbard region: A new model based on revised chronostratigraphy, *Quat. Sci. Rev.*, *28*(9), 812–829.
Knies, J., R. Mattingsdal, K. Fabian, K. Grøsfjeld, S. Baranwal, K. Husum, S. De Schepper, C. Vogt, N. Andersen, and J. Matthiessen (2014), Effect of early Pliocene uplift on late Pliocene cooling in the Arctic-Atlantic gateway, *Earth Planet. Sci. Lett.*, *387*, 132–144.
Luther, A., and G. Axen (2013), Alternating extensional and shortening stress fields on the west Salton detachment fault, Southern California, *Geology*, *41*(10), 1047–1050.
Mattingsdal, R., J. Knies, K. Andreassen, K. Fabian, K. Husum, K. Grøsfjeld, and S. De Schepper (2014), A new 6 Myr stratigraphic framework for the Atlantic-Arctic Gateway, *Quat. Sci. Rev.*, *92*, 170–178.
Moss, J., J. Cartwright, A. Cartwright, and R. Moore (2012), The spatial pattern and drainage cell characteristics of a pockmark field, Nile Deep Sea Fan, *Mar. Pet. Geol.*, *35*(1), 321–336.
Osborne, M. J., and R. E. Swarbrick (1997), Mechanisms for generating overpressure in sedimentary basins: A reevaluation, *AAPG Bull.*, *81*(6), 1023–1041.
Pape, T., P. Geprägs, S. Hammerschmidt, P. Wintersteller, J. Wei, T. Fleischmann, G. Bohrmann, and A. J. Kopf (2014), Hydrocarbon seepage and its sources at mud volcanoes of the Kumano forearc basin, Nankai Trough subduction zone, *Geochem. Geophys. Geosyst.*, doi:10.1002/2013GC005057.
Petersen, C. J., S. Bünz, S. Hustoft, J. Mienert, and D. Klaeschen (2010), High-resolution P-Cable 3D seismic imaging of gas chimney structures in gas hydrated sediments of an Arctic sediment drift, *Mar. Pet. Geol.*, 1–14, doi:10.1016/j.marpetgeo.2010.06.006.
Phrampus, B. J., and M. J. Hornbach (2012), Recent changes to the Gulf Stream causing widespread gas hydrate destabilization, *Nature*, *490*(7421), 527–530.
Planke, S., F. N. Eriksen, C. Berndt, J. Mienert, and D. Masson (2009), Spotlight on technology: P-Cable high-tesolution seismic, *Oceanography*, *22*, 85.
Plaza-Faverola, A., S. Bünz, and J. Mienert (2011), Repeated fluid expulsion through sub-seabed chimneys offshore Norway in response to glacial cycles, *Earth Planet. Sci. Lett.*, *305*(3–4), 297–308.
Plaza-Faverola, A., D. Klaeschen, P. Barnes, I. Pecher, S. Henrys, and J. Mountjoy (2012), Evolution of fluid expulsion and concentrated hydrate zones across the southern Hikurangi subduction margin, New Zealand: An analysis from depth migrated seismic data, *Geochem. Geophys. Geosyst.*, *13*, Q08018, doi:10.1029/2012GC004228.
Plaza-Faverola, A., I. Pecher, G. Crutchley, P. M. Barnes, S. Bünz, T. Golding, D. Klaeschen, C. Papenberg, and J. Bialas (2014), Submarine gas seepage in a mixed contractional and shear deformation regime: Cases from the Hikurangi oblique-subduction margin, *Geochem. Geophys. Geosyst.*, *15*, doi:10.1002/2013GC005082.
Riboulot, V., Y. Thomas, S. Berné, G. Jouet, and A. Cattaneo (2014), Control of Quaternary sea-level changes on gas seeps, *Geophys. Res. Lett.*, *41*, 4970–4977, doi:10.1002/2014GL060460.
Riedel, M., G. D. Spence, N. R. Chapman, and R. D. Hyndman (2002), Seismic investigations of a vent field associated with gas hydrates, offshore Vancouver Island, *J. Geophys. Res.*, *107*(B9), 2200, doi:10.1029/2001JB000269.
Ritzmann, O., W. Jokat, W. Czuba, A. Guterch, R. Mjelde, and Y. Nishimura (2004), A deep seismic transect from Hovgård Ridge to northwestern Svalbard across the continental-ocean transition: A sheared margin study, *Geophys. J. Int.*, *157*(2), 683–702.
Roberts, H. H., and R. S. Carney (1997), Evidence of episodic fluid, gas, and sediment venting on the northern Gulf of Mexico continental slope, *Econ. Geol.*, *92*(7–8), 863.
Roberts, S. J., J. Nunn, L. M. Cathles, and F. Cipriani (1996), Expulsion of abnormally pressured fluids along faults, *J. Geophys. Res.*, *101*(B12), 28,231–28,252, doi:10.1029/96JB02653.

Sahling, H., M. Römer, T. Pape, B. Bergès, C. dos Santos Fereirra, J. Boelmann, P. Geprägs, M. Tomczyk, N. Nowald, and W. Dimmler (2014), Gas emissions at the continental margin west off Svalbard: Mapping, sampling, and quantification, *Biogeosci. Discuss.*, *11*(5), 7189–7234.
Sarkar, S., C. Berndt, A. Chabert, D. G. Masson, T. A. Minshull, and G. K. Westbrook (2011), Switching of a paleo-ice stream in northwest Svalbard, *Quat. Sci. Rev.*, *30*(13), 1710–1725.
Sibson, R. (2000), Tectonic controls on maximum sustainable overpressure: Fluid redistribution from stress transitions, *J. Geochem. Explor.*, *69*, 471–475.
Sibson, R. H. (1990), Conditions for fault-valve behaviour, *Geol. Soc. London Spec. Publ.*, *54*(1), 15–28.
Skarke, A., C. Ruppel, M. Kodis, D. Brothers, and E. Lobecker (2014), Widespread methane leakage from the sea floor on the northern U.S. Atlantic margin, *Nat. Geosci.*, *7*, 657–661, doi:10.1038/ngeo2232.
Smith, A. J., J. Mienert, S. Bünz, and J. Greinert (2014), Thermogenic methane injection via bubble transport into the upper Arctic Ocean from the hydrate-charged Vestnesa Ridge, Svalbard, *Geochem. Geophys. Geosyst.*, *15*, 1945–1959, doi:10.1002/2013GC005179.
Sylvester, A. G. (1988), Strike-slip faults, *Geol. Soc. Am. Bull.*, *100*(11), 1666–1703.
Terakawa, T., Y. Yamanaka, H. Nakamichi, T. Watanabe, F. Yamazaki, S. Horikawa, and T. Okuda (2013), Effects of pore fluid pressure and tectonic stress on diverse seismic activities around the Mt. Ontake volcano, central Japan, *Tectonophysics*, *608*, 138–148.
Vanneste, M., S. Guidard, and J. Mienert (2005), Arctic gas hydrate provinces along the western Svalbard continental margin, *Norw. Petrol. Soc. Spec. Publ.*, *12*, 271–284.
Vogt, P. R., K. Crane, E. Sundvor, M. D. Max, and S. L. Pfirman (1994), Methane-generated (?) pockmarks on young, thickly sedimented oceanic crust in the Arctic: Vestnesa ridge, Fram strait, *Geology*, *22*(3), 255–258.
Vorren, T. O., and J. S. Laberg (1997), Trough mouth fans—palaeoclimate and ice-sheet monitors, *Quat. Sci. Rev.*, *16*(8), 865–881.
Westbrook, G. K., et al. (2009), Escape of methane gas from the seabed along the west Spitsbergen continental margin, *Geophys. Res. Lett.*, *36*, L15608, doi:10.1029/2009GL039191.
Zoback, M. L., M. D. Zoback, J. Adams, M. Assumpcao, S. Bell, E. Bergman, P. Blümling, N. Brereton, D. Denham, and J. Ding (1989), Global patterns of tectonic stress, *Nature*, *341*, 291–298, doi:10.1038/341291a0.
Zühlsdorff, L., and V. Spiess (2004), Three-dimensional seismic characterization of a venting site reveals compelling indications of natural hydraulic fracturing, *Geology*, *32*(2), 101–104.